An Efficient mmWave MIMO Transmission with Hybrid Precoding

Ying Liu[1*], Jinhong Bian[1], and Yuanyuan Wang[1]
[1] School of Information Technology, Yancheng Institute of Technology, Yancheng, 224051, China.
[e-mail: jjf3@ycit.edu.cn]
[*]Corresponding author: Ying Liu

Abstract

This work investigates the hybrid precoder scheme in a millimeter wave (mmWave) multi-user MIMO system. We study a sum rate maximization scheme by jointly designing the digital precoder and the analog precoder. To handle the non-convex problem, a block coordinate descent (BCD) method is formulated, where the digital precoder is solved by a bisection search and the analog precoder is addressed by the penalty dual decomposition (PDD) alternately. Then, we extend the proposed algorithm to the sub-connected schemes. Besides, the proposed algorithm enjoys lower computational complexity when compared with other benchmarks. Simulation results verify the performance of the proposed scheme and provide some meaningful insight.

Keywords: Hybrid precoder, mmWave communications, penalty dual decomposition.

1. Introduction

In recent years, hybrid beamformer (BF)/precoder has been regarded as a prospective technology for millimeter wave (mmWave) communications [1], since the hardware overhead and power cost for radio frequency (RF) circuit and analog-digital (A/D) converters in fully digital system will be extremely large in mmWave system [2].

Two structures have been proposed for hybrid BF/precoder, e.g., the fully-connected and the sub-connected structures [3], where a manifold optimization (MO) approach was proposed to design the precoder. In particular, hybrid BF/precoder design is generally non-convex and hard to handle, mainly caused by the constant modulus constraint (CMC) of the analog BF/precoder [4]. One effective method is to use the matrix factorization, then minimize the Euclidean distance [5]. For example, [6] exploited the spatial sparse structure of the mmWave channels and proposed an orthogonal matching pursuit (OMP) method. And in [7], a MO based hybrid BF was investigated in the presence of beam-misalignment.

Another approach is to handle the original problem directly. To be specific, in [8] and [9], the precoder in multiple-input multiple-output (MIMO) systems was designed via the majorization-minimization (MM) method. Also, [10] proposed a joint design method based on the matrix monotonic optimization. Furthermore, [11] presented an alternating minimization algorithm. In [12], the authors developed a bisection search method to design the hybrid precoder for mmWave systems. In [13], a hybrid BF algorithm was proposed based on the penalty constraint convex concave procedure (CCCP) method. In addition, a neural network scheme was studied to design the hybrid BF [14].

Moreover, [15] investigated a robust hybrid BF technique to resist directions of arrival (DOAs) estimation error. The key idea is to employ null space projection (NSP) in the analog BF. The simulation results showed that the proposed scheme performs more robustly than other baselines. [16] studied the secure hybrid BF scheme in a wiretap channel, where a leakage-based low-complexity algorithm was proposed to design the hybrid BF. Then, in [17], the authors investigated the secure hybrid BF for a mmWave extended reality communications system, where a gradient descent algorithm was proposed to obtain the digital BF and a MM-based scheme is proposed to optimize the analog BF.

These above works mainly focus on the multiple-input single-output (MISO) channel or single user MIMO channel, for more complex mmWave multi-user MIMO (MU-MIMO) channel, [18] proposed a hybrid precoder scheme with quality of service (QoS) constraint. Recently, [19] studied a hybrid precoder scheme for mmWave wiretap channel with the aid of an intelligent reflecting surface (IRS). While in [20], the authors proposed a hybrid BF scheme for sub-connected hybrid precoder structures by using the alternating optimization.

Overall, the optimization methods in these works are computational complex, and some approaches can only suitable for fully-connected scheme or sub-connected scheme. To make the hybrid (BF)/precoder technique more practical, it is important to design a unified method for the two schemes with acceptable computational complexity. Motivated by this fact, we study the hybrid precoder scheme in mmWave multi-user MIMO system in the work, where a weighted sum rate (WSR) objective is solved. Specifically, to obtain the hybrid precoder in the fully-connected scheme, we transform the nonconvex objective function by the MM and block coordinate descent (BCD) methods. Then, the digital precoder is solved via the bisection search and the analog counterpart is solved via the penalty dual decomposition (PDD) technique. Besides, we extend the proposed algorithm to the sub-connected scheme by using the idea of block design. The main contributions are summarized as follows:

a) To tackle the non-convex WSR problem, we recast the objective function into a convex reformulation by applying the MM technique. Then, we decouple the reformulated problem into several subproblems and propose a BCD method to solve each subproblem iteratively.

b) The digital precoder is obtained via the bisection search. While for the analog precoder, we first propose a PDD algorithm for the fully-connected case. Then, by utilizing the block-diagonal feature, we extend the PDD algorithm to the sub-connected case, where several individual subproblems are solved by the PDD method. In fact, a unified optimization method for the hybrid precoder design is developed.

c) We analyze and compare the computational complexity of the proposed algorithm with other benchmarks, and the result indicates that the proposed design is more computational efficiently. Simulation results demonstrate the performance of the proposed scheme and provide some meaningful insights: 1) the proposed method obtains close performance with other baselines; 2) hybrid precoder obtains closed performance of the fully-digital schemes; 3) fully-connected scheme is super than the sub-connected case.

Notations: Throughout the paper, $\succeq$ means positive semi-definite. $\mathbf{A}^T$, $\mathbf{A}^*$, $\mathbf{A}^H$, $\mathbf{A}^{-1}$, $\mathrm{vec}(\mathbf{A})$, $\mathrm{Tr}(\mathbf{A})$ and $|\mathbf{A}|$ denote the transpose, the conjugate, the conjugate transpose, the inverse, the vectorization, the trace, the determinant of $\mathbf{A}$, respectively. The block-diagonal matrix is denoted as $\mathrm{BLKDiag}(\mathbf{A}_1,...,\mathbf{A}_N)$, with diagonal elements $\mathbf{A}_1,...,\mathbf{A}_N$. $[\mathbf{A}]_{m_1:m_2,n_1:n_2}$ denotes the submatrix consisting of the m_1 to m_2 rows and n_1 to n_2 columns of $\mathbf{A}$, and $[\mathbf{a}]_{m:n}$ is the sub-vector contains the m -th to n -th elements of $\mathbf{a}$.

2. System Model and Problem Formulation

2.1 System Model

We study a MU-MIMO downlink network with one Tx and L users as **Fig. 1**. The set for these users is denoted by $\mathcal{U}=\{U_1,...,U_L\}$. We denote $\mathbf{H}_l \in C^{N_{U,l} \times N_{\mathrm{TX}}}$ as the Tx-to-l -th user channel, where N_{TX} and $N_{U,l}$ denote the antenna numbers of the Tx and the l -th user, respectively.
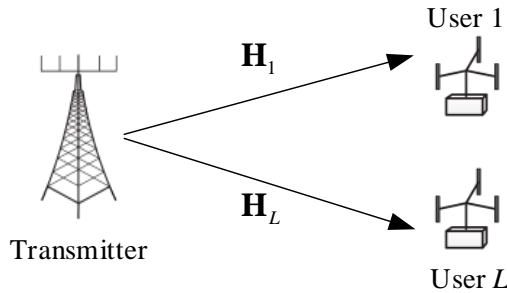

Fig. 1. The system model.

Tx uses $N_{\mathrm{RF}}\,(N_{\mathrm{RF}} \le N_{\mathrm{TX}})$ RF chains to achieve hybrid precoder with two commonly used structures, e.g., the fully-connected structure, where every RF chain is linked to all antennas by N_{TX} phase shifters, and the sub-connected one, where each RF chain is linked to a disjoint subset of antennas by some phase shifters [3].

To improve the system performance, linear precoder is utilized at Tx to transmit the information to all users concurrently. Let $\mathbf{s}_l \in C^{N_{d,l} \times 1}$ denote the symbols for the l-th user. Here, $\mathbf{s}_l$ and $\mathbf{s}_{l'}$ are independent for $l \neq l'$. Then, the transmit signal is

$$\mathbf{x} = \mathbf{F}_a \left(\sum_{l=1}^{L} \mathbf{F}_{d,l} \mathbf{s}_l \right), \tag{1}$$

where $\mathbf{F}_{d,l} \in C^{N_{\mathrm{RF}} \times N_{d,l}}$ represents the digital precoder for the l-th user, while $\mathbf{F}_a \in C^{N_{\mathrm{TX}} \times N_{\mathrm{RF}}}$ is the common analog precoder for all the users. Since $\mathbf{F}_a$ only alters the phase of the signal, $\mathbf{F}_a$ should satisfy the CMC, which is given by $\left| [\mathbf{F}_a]_{m,n} \right| = 1, \forall m, \forall n$. In addition, for the sub-connected scheme, except the CMC, $\mathbf{F}_a$ also need to satisfy the block-diagonal structure $\mathbf{F}_a = \mathrm{BLkDiag}\left[\mathbf{f}_1, \ldots, \mathbf{f}_{N_{\mathrm{RF}}} \right]$, where $\mathbf{f}_r \in C^{N_{\mathrm{TX}}/N_{\mathrm{RF}}}, \forall r \in [1, \ldots, N_{\mathrm{RF}}]$ is a complex vector.

Then, the signal received of the l-th user is

$$\mathbf{y}_l = \mathbf{H}_l \mathbf{F}_a \left(\sum_{l=1}^{L} \mathbf{F}_{d,l} \mathbf{s}_l \right) + \mathbf{n}_l, \forall_l, \tag{2}$$

where $\mathbf{n}_l$ means the noise with $\mathbf{n}_l \sim CN\left(\mathbf{0}, \sigma_l^2 \mathbf{I}\right)$.

The l-th user uses $\mathbf{R}_l \in C^{N_{d,l} \times N_{U,l}}$ to recover $\mathbf{s}_l$. Thus, the rate for the l-th user is

$$R_l = \ln \left| \mathbf{I} + \mathbf{R}_l \mathbf{H}_l \mathbf{F}_a \mathbf{F}_{d,l} \mathbf{F}_{d,l}^H \mathbf{F}_a^H \mathbf{H}_l^H \mathbf{R}_l^H \left(\mathbf{R}_l \mathbf{W}_l \mathbf{R}_l^H \right)^{-1} \right|, \tag{3}$$

where $\mathbf{W}_l = \mathbf{H}_l \mathbf{F}_a \sum_{j \neq l}^{L} \mathbf{F}_{d,j} \mathbf{F}_{d,j}^H \mathbf{F}_a^H \mathbf{H}_l^H + \sigma_l^2 \mathbf{I}$ is the noise plus interference covariance.

Here, we assume that the minimum mean-square error (MMSE) decoder is used by each user, e.g., $\mathbf{R}_l$ is given by

$$\mathbf{R}_l = \mathbf{F}_{d,l}^H \mathbf{F}_a^H \mathbf{H}_l^H \left(\sum_{j=1}^{L} \mathbf{H}_l \mathbf{F}_a \mathbf{F}_{d,j} \mathbf{F}_{d,j}^H \mathbf{F}_a^H \mathbf{H}_l^H + \sigma_l^2 \mathbf{I} \right)^{-1}. \tag{4}$$

Then, (3) is equivalent to

$$R_l = \ln \left| \mathbf{I} + \mathbf{H}_l \mathbf{F}_a \mathbf{F}_{d,l} \mathbf{W}_l^{-1} \mathbf{F}_{d,l}^H \mathbf{F}_a^H \mathbf{H}_l^H \right|, \tag{5}$$

where the proof of (5) can be found in [16, Appendix A].

2.2 Channel Model

According to the Saleh-Valenzuela model [6], [21], [24], $\mathbf{H}_1$ is given by

$$\mathbf{H}_1 = \sum_{p=1}^{N_{\mathrm{path}}} \alpha_p \mathbf{a}_r \left(\psi_p^r, \beta_p^r \right) \mathbf{a}_t \left(\psi_p^t, \beta_p^t \right)^H, \tag{6}$$

where N_{path} is the path number in $\mathbf{H}_1$, $\alpha_p \sim CN\left(0, \kappa^2 10^{-0.1PL(D)}\right)$ is the scale of the p-th path in $\mathbf{H}_1$, $\kappa = \sqrt{M_1 N_{\mathrm{TX}}/N_{\mathrm{path}}}$ and $PL(D)$ denotes the loss [21]. Besides, $\mathbf{a}_r \left(\psi_p^r, \beta_p^r \right) / \mathbf{a}_t \left(\psi_p^t, \beta_p^t \right)$ denote the array responses of the p-th path, where $\psi_p^r \left(\beta_p^r \right) / \psi_p^t \left(\beta_p^t \right)$ is the azimuth (elevation) angles of arrival/departure.

For uniform planar arrays, $\mathbf{a}_t \left(\psi_p^t, \beta_p^t \right)$ is given by

$$\mathbf{a}_t(\psi_p, \beta_p) = \frac{1}{\sqrt{N_{\mathrm{TX}}}} \left[1, \ldots, e^{j\frac{2\pi d}{\lambda}(w\sin(\psi_p)\sin(\beta_p)+h\cos(\beta_p))}, \ldots, e^{j\frac{2\pi d}{\lambda}((W-1)\sin(\psi_p)\sin(\beta_p)+(H-1)\cos(\beta_p))} \right]^T, \tag{7}$$

where λ means the wave length, d denotes the entry space, and $0 \leq w < W$, $0 \leq h < H$ are the entry indices. Thus, the array size is $N_{TX} = WH$.

2.3 Problem Formulation

Mathematically, the WSR design is given as

$$\max_{\{\mathbf{F}_{d,l}\}_{l=1}^{L}, \mathbf{F}_a} \quad \sum_{l=1}^{L} \varpi_l R_l \tag{8a}$$

$$\text{s.t.} \quad \sum_{l=1}^{L} \text{Tr}\left(\mathbf{F}_a \mathbf{F}_{d,l} \mathbf{F}_{d,l}^H \mathbf{F}_a^H\right) \leq P_s, \tag{8b}$$

$$\left|[\mathbf{F}_a]_{m,n}\right| = 1, \forall m, \forall n, \tag{8c}$$

where $\varpi_l \left(0 \leq \varpi_l \leq 1, \sum_{l=1}^{L} \varpi_l = 1\right)$ means the weight for R_l, (8b) is the transmit power constraint with P_s being the maximum transmit power, and (8c) is the unit modules constraint of the analog precoder.

3. Joint Digital and Analog Precoder Design

3.1 Problem Transformation

Firstly, due to the Sylvester's determinant property, i.e., $|\mathbf{I} + \mathbf{MN}| = |\mathbf{I} + \mathbf{NM}|$, we have $R_l = \ln\left|\mathbf{I} + \mathbf{H}_l \mathbf{F}_a \mathbf{F}_{d,l} \mathbf{F}_{d,l}^H \mathbf{F}_a^H \mathbf{H}_l^H \mathbf{W}_l^{-1}\right|$.

Then, we aim to find a lower bound of R_l. According to [22], we denote

$$\mathbf{D}_l = \begin{bmatrix} \mathbf{I}_M & \mathbf{F}_{d,l}^H \mathbf{F}_a^H \mathbf{H}_l^H \\ \mathbf{H}_l \mathbf{F}_a \mathbf{F}_{d,l} & \mathbf{H}_l \mathbf{F}_a \mathbf{F}_{d,l} \mathbf{F}_{d,l}^H \mathbf{F}_a^H \mathbf{H}_l^H + \mathbf{W}_l \end{bmatrix}. \tag{9}$$

Via the method in [22], we obtain the following lower bound of

$$R_l \geq \ln\left|\mathbf{E}\bar{\mathbf{D}}_l^{-1}\mathbf{E}\right| - \text{Tr}\left(\bar{\mathbf{C}}_l\left(\mathbf{D}_l - \bar{\mathbf{D}}_l\right)\right), \tag{10}$$

where $\mathbf{E} = [\mathbf{I}_M \ \mathbf{0}]^T$, $\bar{\mathbf{D}}_l$ is the obtained $\mathbf{D}_l$ in the previous iteration, and $\bar{\mathbf{C}}_l$ is given by $\bar{\mathbf{C}}_l = \bar{\mathbf{D}}_l^{-1}\mathbf{E}\left(\mathbf{E}^H\bar{\mathbf{D}}_l^{-1}\mathbf{E}\right)^{-1}\mathbf{E}^H\bar{\mathbf{D}}_l^{-1}$.

Then, by denoting $\bar{c}_l = \ln\left|\mathbf{E}^H\bar{\mathbf{D}}_l^{-1}\mathbf{E}\right| + \text{Tr}\left(\bar{\mathbf{C}}_l\bar{\mathbf{D}}_l\right)$, we attain $R_l \geq \bar{c}_l - \text{Tr}\left(\bar{\mathbf{C}}_l\mathbf{D}_l\right)$ and solve the following problem

$$\min_{\{\mathbf{F}_{d,l}\}_{l=1}^{L}, \mathbf{F}_a} \quad \varpi_l \text{Tr}\left(\bar{\mathbf{C}}_l \mathbf{D}_l\right) \tag{11a}$$

$$\text{s.t.} \quad (8b), (8c). \tag{11b}$$

Moreover, we denote $\bar{\mathbf{F}}_a$ and $\bar{\mathbf{F}}_{d,l}$ as the obtained $\mathbf{F}_a$ and $\mathbf{F}_{d,l}$ in the previous iteration, and $\bar{\mathbf{W}}_l = \mathbf{H}_l \sum_{j \neq l}^{L} \bar{\mathbf{F}}_a \bar{\mathbf{F}}_{d,j} \bar{\mathbf{F}}_{d,j}^H \bar{\mathbf{F}}_a^H \mathbf{H}_l^H + \sigma_l^2 \mathbf{I}$. Then, according to [22], $\bar{\mathbf{C}}_l$ can be decomposed as

$$\overline{\mathbf{C}}_l = \begin{bmatrix} \mathbf{C}_l^{11} & \mathbf{C}_l^{12} \\ \mathbf{C}_l^{21} & \mathbf{C}_l^{22} \end{bmatrix} = \begin{bmatrix} \overline{\mathbf{P}}_l^H & \overline{\mathbf{Q}}_l \\ \overline{\mathbf{Q}}_l^H & \overline{\mathbf{Q}}_l^H \overline{\mathbf{P}}_l^{-1} \overline{\mathbf{Q}}_l \end{bmatrix}. \tag{12}$$

where $\overline{\mathbf{P}}_l$ and $\overline{\mathbf{Q}}_l$ are, respectively, given by

$$\overline{\mathbf{P}}_l = \mathbf{I} + \overline{\mathbf{F}}_{d,l}^H \overline{\mathbf{F}}_a^H \mathbf{H}_l^H \overline{\mathbf{W}}_l^{-1} \mathbf{H}_l \overline{\mathbf{F}}_a \overline{\mathbf{F}}_{d,l}, \tag{13a}$$

$$\overline{\mathbf{Q}}_l = -\overline{\mathbf{F}}_{d,l}^H \overline{\mathbf{F}}_a^H \mathbf{H}_l^H \overline{\mathbf{W}}_l^{-1}. \tag{13b}$$

Thus, we have

$$\overline{\mathbf{C}}_l \mathbf{D}_l = \mathbf{C}_l^{11} + 2\Re\left\{\mathbf{A}_l^{12} \mathbf{H}_l \mathbf{F}_a \mathbf{F}_{d,l}\right\} + \mathbf{C}_l^{22} + \sigma_l^2 \mathbf{C}_l^{22} \mathbf{H}_l \mathbf{F}_a \left(\sum_{l=1}^L \mathbf{F}_{d,l} \mathbf{F}_{d,l}^H\right) \mathbf{F}_a^H \mathbf{H}_l^H. \tag{14}$$

Via the above procedure, the WSR design is transformed to

$$\min_{\{\mathbf{F}_{d,l}\}_{l=1}^L, \mathbf{F}_a} \sum_{l=1}^L 2\varpi_l \Re\left\{\mathrm{Tr}\left(\mathbf{C}_l^{12} \mathbf{H}_l \mathbf{F}_a \mathbf{F}_{d,l}\right)\right\} + \sum_{l=1}^L \varpi_l \mathrm{Tr}\left(\mathbf{C}_l^{22} \mathbf{H}_l \mathbf{F}_a \left(\sum_{l=1}^L \mathbf{F}_{d,l} \mathbf{F}_{d,l}^H\right) \mathbf{F}_a^H \mathbf{H}_l^H\right) \tag{15a}$$

$$\text{s.t. } (8b),(8c). \tag{15b}$$

When fixing other variables, (15a) is quadratic with respect to (w.r.t.) the specific variable.

3.2 Digital Precoder Optimization

By denoting $\mathbf{f}_{d,l} = \mathrm{vec}(\mathbf{F}_{d,l})$ and utilizing the vectorization operation, i.e., $\mathrm{Tr}(\mathbf{ST}) = \mathrm{vec}(\mathbf{S}^H)^H \mathrm{vec}(\mathbf{T})$ and $\mathrm{Tr}(\mathbf{U}^H \mathbf{VWX}) = \mathrm{vec}(\mathbf{U})^H (\mathbf{X}^T \otimes \mathbf{V}) \mathrm{vec}(\mathbf{W})$, (15a) is recast as

$$\min_{\{\mathbf{f}_{d,l}\}_{l=1}^L} \sum_{l=1}^L \left(\mathbf{f}_{d,l}^H \mathbf{V} \mathbf{f}_{d,l} + 2\Re\left\{\mathbf{v}_l^H \mathbf{f}_{d,l}\right\}\right) \tag{16}$$

where $\mathbf{V} = \mathbf{I} \otimes \left(\sum_{l=1}^L \varpi_l \mathbf{F}_a^H \mathbf{H}_l^H \mathbf{A}_l^{22} \mathbf{H}_l \mathbf{F}_a\right)$ and $\mathbf{v}_l = \varpi_l \mathrm{vec}\left(\left(\mathbf{A}_l^{12} \mathbf{H}_l \mathbf{F}_a\right)^H\right)$, respectively.

Thus, we have

$$\min_{\{\mathbf{f}_{d,l}\}_{l=1}^L} \sum_{l=1}^L \left(\mathbf{f}_{d,l}^H \mathbf{V} \mathbf{f}_{d,l} + 2\Re\left\{\mathbf{v}_l^H \mathbf{f}_{d,l}\right\}\right) \tag{17a}$$

$$\text{s.t. } \sum_{l=1}^L \mathbf{f}_{d,l}^H \left(\mathbf{F}_a^H \mathbf{F}_a \otimes \mathbf{I}\right) \mathbf{f}_{d,l} \leq P_s. \tag{17b}$$

Then, the Lagrange function is

$$\mathcal{L}\left(\{\mathbf{f}_{d,l}\}_{l=1}^L, u\right) = \sum_{l=1}^L \left(\mathbf{f}_{d,l}^H \mathbf{V} \mathbf{f}_{d,l} + 2\Re\left\{\mathbf{v}_l^H \mathbf{f}_{d,l}\right\}\right) + u\left(\sum_{l=1}^L \mathbf{f}_{d,l}^H \left(\mathbf{F}_a^H \mathbf{F}_a \otimes \mathbf{I}\right) \mathbf{f}_{d,l} - P_s\right), \tag{18}$$

where $u \geq 0$ is the dual variable of (17b).

Therefore, we obtain

$$g(u) = \min_{\{\mathbf{f}_{d,l}\}_{l=1}^L} \mathcal{L}\left(\{\mathbf{f}_{d,l}\}_{l=1}^L, u\right), \tag{19}$$

and the dual problem is

$$\max_{u} \ g(u) \ \text{s.t.} \ u \geq 0. \tag{20}$$

Given u, we denote the optimal solution to (19) as $\{\mathbf{f}_{d,l}(u)\}_{l=1}^{L}$. Then, based on the first-order optimization condition w.r.t. $\mathbf{f}_{d,l}$, the optimal $\mathbf{f}_{d,l}$ is given by

$$\mathbf{f}_{d,l}(u) = -\left(u\mathbf{F}_a^H\mathbf{F}_a \otimes \mathbf{I} + \mathbf{V}\right)^{-1}\mathbf{v}_l. \tag{21}$$

The optimal u should satisfy the complementary slackness constraint

$$u\left(\sum_{l=1}^{L}\mathbf{f}_{d,l}^H(u)\left(\mathbf{F}_a^H\mathbf{F}_a \otimes \mathbf{I}\right)\mathbf{f}_{d,l}(u) - P_s\right) = 0. \tag{22}$$

From (22), the optimal u can be determined by the following procedure: if $u = 0$ and the constraint

$$\sum_{l=1}^{L}\mathbf{f}_{d,l}^H(0)\left(\mathbf{F}_a^H\mathbf{F}_a \otimes \mathbf{I}\right)\mathbf{f}_{d,l}(0) \leq P_s, \tag{23}$$

is satisfied, then the optimal u is $u = 0$. Otherwise, we need to find the optimal u by solving

$$P(u) = \sum_{l=1}^{L}\mathbf{f}_{d,l}^H(u)\left(\mathbf{F}_a^H\mathbf{F}_a \otimes \mathbf{I}\right)\mathbf{f}_{d,l}(u) = P_s. \tag{24}$$

In fact, [23] have proved that $P(u)$ is decreasing w.r.t. u monotonically, thus u can be obtained by bisection search. The whole bisection search is summarized as Algorithm 1.

Algorithm 1: Bisection search algorithm

1: Set the accuracy threshold ε and the bounds u_l, u_u;

2: Calculate $\{\mathbf{f}_{d,l}(0)\}_{l=1}^{L}$ by (21). If u satisfying (23), then $u^* = 0$. Otherwise, execute the following steps;

3: **Repeat**

4:    Calculate $u = (u_l + u_u)/2$;

5:    Obtain $\{\mathbf{f}_{d,l}(u)\}_{l=1}^{L}$ by (21)

6:    Calculate $P(u)$ by (24). If $P(u) \geq P_s$, set $u_l = u$. Otherwise, set $u_u = u$;

7: **Until** $|u_l - u_u| \leq \varepsilon$

8: **Output** $\left(u^*, \{\mathbf{F}_{d,l}^*\}_{l=1}^{L}\right)$.

3.3 Analog Precoder Optimization

Here, we optimize the analog precoder $\mathbf{F}_a$, where the method is mainly based on the PDD algorithm.

3.3.1 The Fully-Connected Analog Precoder Design

This problem is given by

$$\min_{\mathbf{F}_a} \ \sum_{l=1}^{L}2\varpi_l\Re\left\{\text{Tr}\left(\mathbf{A}_l^{12}\mathbf{H}_l\mathbf{F}_a\mathbf{F}_{d,l}\right)\right\} + \sum_{l=1}^{L}\varpi_l\text{Tr}\left(\mathbf{A}_l^{22}\mathbf{H}_l\mathbf{F}_a\left(\sum_{l=1}^{L}\mathbf{F}_{d,l}\mathbf{F}_{d,l}^H\right)\mathbf{F}_a^H\mathbf{H}_l^H\right) \tag{25a}$$

$$\text{s.t. (8b)}, \left|\left[\mathbf{F}_a\right]_{m,n}\right| = 1, \forall m, \forall n. \tag{25b}$$

Via denoting $\mathbf{f}_a = \text{vec}(\mathbf{F}_a)$, (25) is equivalent to

$$\min_{\mathbf{f}_a} \quad f\left(\mathbf{f}_a\right) = \mathbf{f}_a^H \mathbf{\Omega} \mathbf{f}_a + 2\Re\left\{\boldsymbol{\omega}^H \mathbf{f}_a\right\} \tag{26a}$$

$$\text{s.t. } \mathbf{f}_a^H \left(\sum_{l=1}^L \mathbf{F}_{d,l}^H \mathbf{F}_{d,l} \otimes \mathbf{I}\right) \mathbf{f}_a \leq P_s, \tag{26b}$$

$$\left|\left[\mathbf{f}_a\right]_n\right| = 1, \forall n, \tag{26c}$$

where $\mathbf{\Omega} = \sum_{l=1}^L \left(\sum_{l=1}^L \mathbf{F}_{d,l} \mathbf{F}_{d,l}^H\right)^T \otimes \varpi_l \mathbf{H}_l^H \mathbf{A}_l^{22} \mathbf{H}_l$ and $\boldsymbol{\omega} = \sum_{l=1}^L \varpi_l \text{vec}\left(\left(\mathbf{F}_{d,l} \mathbf{A}_l^{12} \mathbf{H}_l\right)^H\right)$, respectively.

Next, we handle (26). At first, we introduce $\mathbf{z} \in C^{N_{TX}N_{RF} \times 1}$ and recast (26) as

$$\min_{\mathbf{f}_a, \mathbf{z}} \mathbf{f}_a^H \mathbf{\Omega} \mathbf{f}_a + 2\Re\left\{\boldsymbol{\omega}^H \mathbf{f}_a\right\} \tag{27a}$$

$$\text{s.t. } \mathbf{f}_a^H \left(\sum_{l=1}^L \mathbf{F}_{d,l}^H \mathbf{F}_{d,l} \otimes \mathbf{I}\right) \mathbf{f}_a \leq P_s, \tag{27b}$$

$$\mathbf{f}_a = \mathbf{z}, \tag{27c}$$

$$\left|\left[\mathbf{z}\right]_n\right| = 1, \forall n. \tag{27d}$$

Then, by penalizing (27c), we obtain

$$\min_{\mathbf{f}_a, \mathbf{z}, \mathbf{t}} \mathbf{f}_a^H \mathbf{\Omega} \mathbf{f}_a + 2\Re\left\{\boldsymbol{\omega}^H \mathbf{f}_a\right\} + \frac{1}{2\lambda}\left\|\mathbf{f}_a - \mathbf{z}\right\|_2^2 + \Re\left\{\mathbf{t}^H\left(\mathbf{f}_a - \mathbf{z}\right)\right\} \tag{28a}$$

$$\text{s.t. } \left(27b\right), \left(27d\right), \tag{28b}$$

where $\lambda \geq 0$ and $\mathbf{t} \in C^{N_{TX}N_{RF} \times 1}$ are the penalty factor and the dual variable of (27c).

The PDD consists of a two-layer optimization. Specifically, for the inner layer iteration, when $\mathbf{z}$ is fixed, (28) is recast as

$$\min_{\mathbf{f}_a} \mathbf{f}_a^H \mathbf{\Omega} \mathbf{f}_a + 2\Re\left\{\boldsymbol{\omega}^H \mathbf{f}_a\right\} + \frac{1}{2\lambda}\left\|\mathbf{f}_a - \mathbf{z}\right\|_2^2 + \Re\left\{\mathbf{t}^H\left(\mathbf{f}_a - \mathbf{z}\right)\right\} \tag{29a}$$

$$\text{s.t. } \left(27b\right), \tag{29b}$$

which is convex and can be solved by bisection search.

Then, when $\mathbf{f}_a$ is given, we have

$$\min_{\mathbf{z}} \frac{1}{2\lambda}\left\|\mathbf{f}_a - \mathbf{z}\right\|_2^2 + \Re\left\{\mathbf{t}^H\left(\mathbf{f}_a - \mathbf{z}\right)\right\} \tag{30a}$$

$$\text{s.t. } \left|\left[\mathbf{z}\right]_n\right| = 1, \forall n. \tag{30b}$$

Due to (30b), we have $\frac{1}{2\lambda}\left\|\mathbf{z}\right\|_2^2 = \frac{N_{TX}N_{RF}}{2\lambda}$. Hence, (30) is simplified to

$$\max_{\left|[\mathbf{z}]_n\right|=1} \Re\left\{\left(\mathbf{f}_a + \lambda\mathbf{t}\right)^H \mathbf{z}\right\}, \tag{31}$$

and the optimal solution is $\mathbf{z} = e^{j\angle\left(\mathbf{f}_a + \lambda\mathbf{t}\right)}$.

The inner layer updates $\mathbf{f}_a$ and $\mathbf{z}$ until convergence alternatively. As for the outer layer, $\mathbf{t}$ and λ are updated by $\mathbf{t} \leftarrow \mathbf{t} + \lambda^{-1}(\mathbf{f}_a - \mathbf{z})$ and $\lambda \leftarrow \rho\lambda$, where $\rho \leq 1$ is the scaling factor to control λ.

Algorithm 2: PDD algorithm

1: Initialize $\{\mathbf{f}_a^0, \mathbf{z}^0, \mathbf{t}^0, \lambda^0\}$ and set $i = 1$;

2: **Repeat**

3:   set $\mathbf{f}_a^{i-1,l} = \mathbf{f}_a^{i-1}$, $\mathbf{f}_a^{i-1,l} = \mathbf{f}_a^{i-1}$, $l = 0$;

4:   **Repeat**

5:     Updating $\mathbf{f}_a^{i-1,l+1}$ by solving (29);

6:     Updating $\mathbf{z}^{i-1,l+1}$ by $\mathbf{z} = e^{j\angle(\mathbf{f}_a + \lambda\mathbf{t})}$, $l \leftarrow l+1$;

7:   **Until Convergence**

8:   Set $\mathbf{f}_a^i = \mathbf{f}_a^{i-1,l}$, $\mathbf{z}^i = \mathbf{z}^{i-1,l}$;

9:   **If** $\left\| \mathbf{f}_a^i - \mathbf{z}^i \right\|_2 \leq v^i$, **then** $\mathbf{t}^{i+1} = \mathbf{t}^i + \frac{1}{\lambda^i}(\mathbf{f}_a^i - \mathbf{z}^i)$, $\lambda^{i+1} = \lambda^i$;

10:   **else** $\mathbf{t}^{i+1} = \mathbf{t}^i$, $\lambda^{i+1} = c\lambda^i$; **end**

11:   $i \leftarrow i+1$;

12: **Until** $\left\| \mathbf{f}_a^l - \mathbf{z}^l \right\|_2 \leq \varepsilon$;

Since the convergence of PDD have been proved in [18, Appendix A], we omit this for brevity.

3.3.2 The Sub-Connected Analog Precoder Design

Firstly, we define $b = N_{\text{TX}}/N_{\text{RF}}$. Due to the block diagonal structures of $\mathbf{F}_a$, we have

$$2\varpi_l \Re\left\{ \text{Tr}\left(\mathbf{A}_l^{12}\mathbf{H}_l\mathbf{F}_a\mathbf{F}_{d,l}\right)\right\} = \sum_{r=1}^{N_{\text{RF}}}\left\{ 2\varpi_l \Re\left\{ \text{Tr}\left(\left[\mathbf{A}_l^{12}\mathbf{H}_l\right]_{:,(r-1)b+1:rb}\mathbf{f}_r\left[\mathbf{F}_{d,l}\right]_{r,:}\right)\right\}\right\}, \tag{32}$$

and

$$\varpi_l \text{Tr}\left(\mathbf{A}_l^{22}\mathbf{H}_l\mathbf{F}_a\left(\sum_{l=1}^{L}\mathbf{F}_{d,l}\mathbf{F}_{d,l}^H\right)\mathbf{F}_a^H\mathbf{H}_l^H\right)$$

$$= \sum_{r=1}^{N_{\text{RF}}}\left\{ \varpi_l \text{Tr}\left(\left[\mathbf{A}_l^{22}\mathbf{H}_l\right]_{:,(r-1)b+1:rb}\mathbf{f}_r\left[\left(\sum_{l=1}^{L}\mathbf{F}_{d,l}\mathbf{F}_{d,l}^H\right)\right]_{r,r}\times\mathbf{f}_r^H\left[\mathbf{H}_l^H\right]_{(r-1)b+1:rb,:}\right)\right\}. \tag{33}$$

Thus, the following equations hold

$$\sum_{l=1}^{L} 2\varpi_l \Re\left\{ \text{Tr}\left(\mathbf{A}_l^{12}\mathbf{H}_l\mathbf{F}_a\mathbf{F}_{d,l}\right)\right\} = \sum_{r=1}^{N_{\text{RF}}} 2\Re\left\{\mathbf{w}_r^H\mathbf{f}_r\right\}, \tag{34a}$$

$$\sum_{l=1}^{L} \varpi_l \text{Tr}\left(\mathbf{A}_l^{22}\mathbf{H}_l\mathbf{F}_a\left(\sum_{l=1}^{L}\mathbf{F}_{d,l}\mathbf{F}_{d,l}^H\right)\mathbf{F}_a^H\mathbf{H}_l^H\right) = \sum_{r=1}^{N_{\text{RF}}}\mathbf{f}_r^H\mathbf{W}_r\mathbf{f}_r, \tag{34b}$$

where

$$\mathbf{w}_r^H = \sum_{l=1}^{L} \varpi_l \left[\mathbf{F}_{d,l} \right]_{r,:} \left[\mathbf{A}_l^{12} \mathbf{H}_l \right]_{:,(r-1)s+1:rs}, \tag{35a}$$

$$\mathbf{W}_r = \sum_{l=1}^{L} \left\{ \varpi_l \left[\left(\sum_{l=1}^{L} \mathbf{F}_{d,l} \mathbf{F}_{d,l}^H \right) \right]_{r,r} \times \left[\mathbf{H}_l^H \right]_{(r-1)s+1:rs,:} \left[\mathbf{A}_l^{22} \mathbf{H}_l \right]_{:,(r-1)s+1:rs} \right\}. \tag{35b}$$

Thus, by neglecting (8b), we obtain

$$\min_{\mathbf{f}_r} \sum_{r=1}^{N_{RF}} \left\{ \mathbf{f}_r^H \mathbf{W}_r \mathbf{f}_r + 2\Re \left\{ \mathbf{w}_r^H \mathbf{f}_r \right\} \right\} \tag{36a}$$

$$\text{s.t. } \left| \left[\mathbf{f}_r \right]_n \right| = 1, \forall n \in [1, \dots, s]. \tag{36b}$$

Since for different $r \neq r'$, $\mathbf{f}_r$ and $\mathbf{f}_{r'}$ are independent, (36) can be treated as N_{RF} minimization subproblems. Then, the previous proposed PDD algorithm can be applied to the sub-connected case, from $r = 1$ to $r = N_{RF}$ until all the columns in $\mathbf{F}_a$ are optimized.

3.4 Overall Algorithm and Complexity Analysis

Algorithm 3: BCD algorithm

1: Initialize $\left(\mathbf{F}_{d,l}^0, \mathbf{F}_a^0 \right)$, choose $\rho > 0$ and set $k = 0$;

2: **Repeat**

3:　Obtain $\mathbf{F}_{d,l}^k$ via solving (17);

4:　Obtain $\mathbf{F}_a^k$ via solving (26) or (36);

5:　Update $\mathbf{H}_l$, $\mathbf{C}_l^{11}$, $\mathbf{C}_l^{12}$ 和 $\mathbf{C}_l^{22}$;

6:　$k \leftarrow k + 1$

7: **Until terminate**;

8: **Output** $\left(\mathbf{F}_{d,l}^\star, \mathbf{F}_a^\star \right)$.

The BCD algorithm is summarized as Algorithm 3. Besides, the complexity to optimize $\left\{ \mathbf{F}_{d,l} \right\}_{l=1}^{L}$ is given by $\mathcal{O}\left(\log_2 \left(\frac{u_u - u_l}{\varepsilon} \right) \sum_{l=1}^{L} N_{d,l}^2 N_{RF}^2 \right)$. As for the PDD algorithm to update $\mathbf{f}_a$, the main complexity is given by $\mathcal{O}\left(T \left(N_{TX} N_{RF} + 1 \right)^2 \right)$, where T is the iteration number. Thus, the overall complexity is

$$\mathcal{C} = O\left(\max \left\{ \log_2 \left(\frac{u_u - u_l}{\varepsilon} \right) \sum_{l=1}^{L} N_{d,l}^2 N_{RF}^2, T \left(N_{TX} N_{RF} + 1 \right)^2 \right\} \right), \tag{37}$$

which is polynomial time.

In addition, we have mentioned that one can use the bisection method to handle (29). For (29), if the bisection method is used to obtain $\mathbf{f}_a$, the computational complexity is given by

$$\mathcal{C} = O\left(\log_2 \left(\frac{u_u - u_l}{\varepsilon} \right) N_{TX}^2 N_{RF}^2 \right), \tag{38}$$

which is a quadratic function w.r.t. the dimension of $\mathbf{f}_a$. Therefore, it is suitable for a practical scenario when the dimension of $\mathbf{f}_a$ is large.

Moreover, we noted that the complexity of the MMSE-based method in [11] is

$$\mathcal{C} = O\left(N_{\text{out}} N_{\text{in}} \left(4N_{\text{TX}}^2 N_{\text{RF}} + 13 N_{\text{TX}} N_{\text{RF}}^2 + 4 N_{\text{RF}}^3\right)\right), \tag{39}$$

where N_{out} and N_{in} are the iteration numbers.

While the complexity of the local-optimal method in [20] is

$$\mathcal{C} = O\left(I_{\text{P}}\left(I_{\text{A}}\left(\frac{5}{3}N_{\text{TX}}^3 + (L+1)N_{\text{TX}}^2\right)\right) + (L+2)\left(N_{\text{TX}}^2 + N_{\text{RF}}^2\right)\right), \tag{40}$$

where I_{P} and I_{A} are the iteration numbers.

From the comparison, we can see that the proposed method is more computational efficiently than these benchmarks since $N_{d,l}$ and N_{RF} are commonly much smaller than these iteration numbers. Readers can refer [11] and [20] for more detail about $\{N_{\text{out}}, N_{\text{in}}, I_{\text{P}}, I_{\text{A}}\}$.

4. Simulation Results

We set the coordinates of Tx as $(10\,\text{m}, 0\,\text{m}, 20\,\text{m})$, and set the 5 users in a circle with radius $5\,\text{m}$ and centered at $(10\,\text{m},\ 50\,\text{m},\ 1.5\,\text{m})$ randomly. Unless specified, we set $N_{\text{TX}} = 4 \times 4$, $N_{d,l} = 8$, $N_{U,l} = 2 \times 2$, $\varpi_l = 1/L, \forall l$, and $P_s = 30\,\text{dBm}$, $\sigma_l^2 = -80\,\text{dBm}, \forall l$. In addition, we assume $N_{\text{path}} = 8$, and $PL(D)$ is [24]:

$$PL(D)[\text{dB}] = a + 10b\log_{10}(D) + \zeta, \tag{41}$$

where $\zeta \sim N(0, \varrho^2)$.

4.1 Convergence

Specifically, the PDD method is referred as the inner layer iteration and the BCD method is referred as the outer layer iteration.

Fig. 2 provides the convergence of the former, where the solid and dotted lines denote the fully-and-sub-connected cases, respectively. From this figure, we observe that the WSR increase with the iteration numbers for different N_{TX} and N_{RF}, and converge within 40 iterations, which demonstrates the convergence.
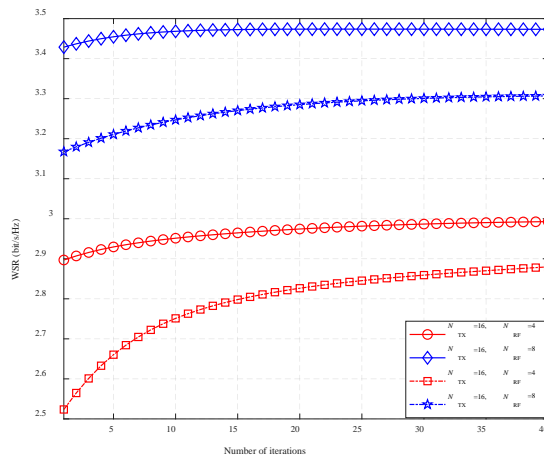

Fig. 2. PDD algorithm convergence.

Then, we test the convergence of the latter in **Fig. 3** and **4**, for the fully-and sub-connected cases, respectively. From the two figures, we can see that the WSR increases and finally converges within 20 iterations for various N_{TX} and N_{RF}. Besides, by comparing the two figures, we can see that in the same channel condition, the fully-connected scheme overwhelms the sub-connected case.
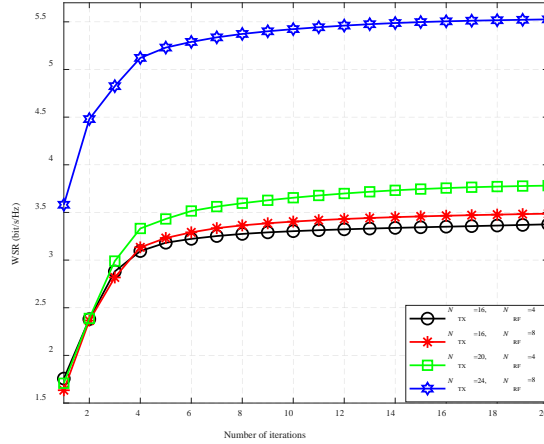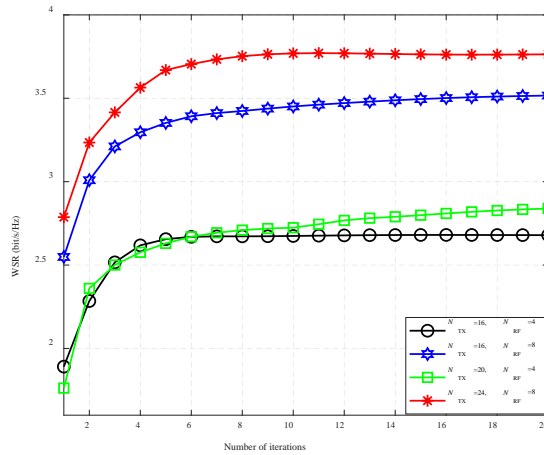

Fig. 3. BCD algorithm convergence: Fully-connected case.

Fig. 4. BCD algorithm convergence: Sub-connected case.

4.2 Performance Evaluation

We evaluate the performance of these schemes, which are labeled as "Fully-connected case", "Sub-connected case", and "Fully digital precoder", respectively. In addition, we compare the proposed method with some other benchmarks: 1) the MMSE method in [11], which is used for the fully-connected case and is labeled as "MMSE method"; 2) the local-optimal method in [20], which is used for the sub-connected case and is labeled as "Local-optimal method", respectively.

At first, **Fig. 5** plots the WSR and P_s, where we can see that the fully digital precoder obtain a performance improvement than that of the hybrid precoder, at the cost of high implementation complexity. Since we assume $N_{\mathrm{RF}} = 4$ RF chains in this simulation, e.g., only

a quarter of N_{TX}, thus the hybrid precoder inevitable suffer a certain performance loss, especially for the sub-connected hybrid precoder. Besides, we can see that the proposed method obtains close performance with the methods in [11] and [20], both for the fully-connected case and sub-connected case.
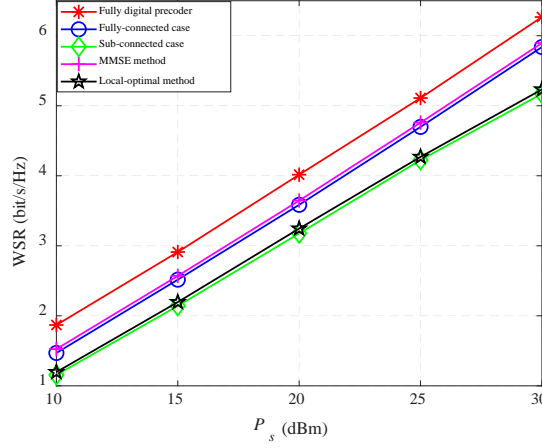

Fig. 5. WSR versus P_s.

Then, we plot the WSR versus N_{TX} in **Fig. 6**. As we can see, with larger N_{TX}, a more spatial degrees of freedom (DoF) can be obtained by these methods, thus is beneficial to improve the WSR. Besides, the gap among the fully digital case and the hybrid scheme is slightly enlarged with N_{TX}, since the performance of the latter is not only affected by N_{TX}, but also constrained by N_{RF}.
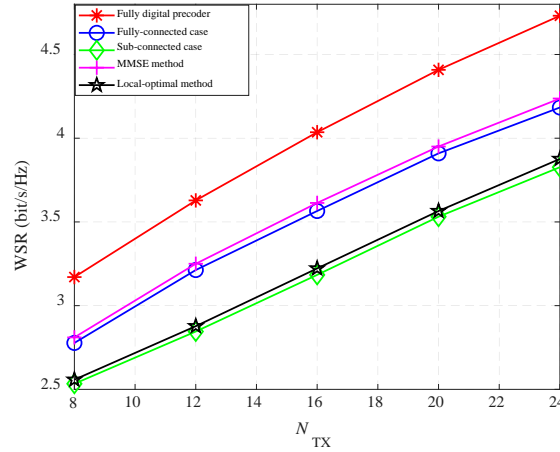

Fig. 6. WSR versus N_{TX}.

Next, we plot the WSR versus N_{RF} in **Fig. 7**, where we can see that the WSR increases with N_{RF} for all these hybrid methods, since the extra RF chain can facilitate the exploration of the spatial DoF. In addition, when $N_{\text{RF}} = N_{\text{TX}}$, the fully-connected hybrid precoder obtains closed performance as the fully digital scheme, which shows the availability of the former.
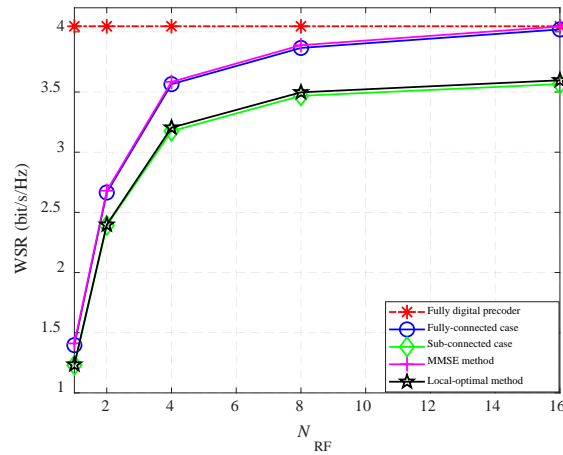
Fig. 7. The WSR versus N_{RF}.

Lastly, as pointed by [12], energy efficiency is an important criterion of wireless communication. Motivated by this, we generate the method to the energy efficiency design by adopting the Dinkelbach's method [25]. From **Fig. 8**, one observes that for all these schemes, the efficiency tends to converge to a constant when P_s becomes large. Since there exists a unique P_s for the energy efficiency maximization. Besides, we observe that the sub-connect method outperforms others schemes due to its simplest structure, while the fully digital precoder method leads to the worst performance due to the fully digital structure, which lead to the highest circuit power consumption, thus reduces the energy efficiency.
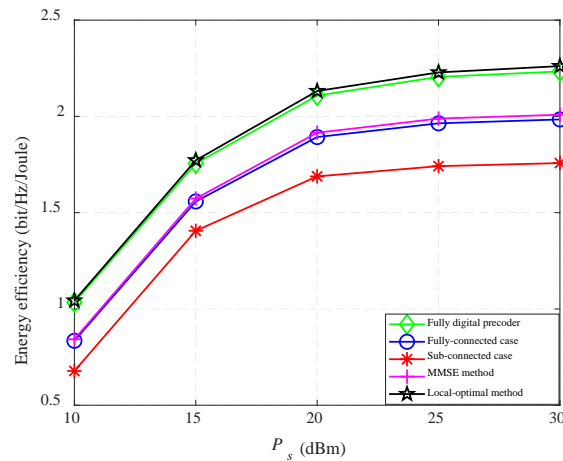

Fig. 8. The energy efficiency versus P_s.

5. Conclusion

This work developed a unified hybrid precoder design in a mmWave multi-user MIMO system. Specifically, we studied the WSR design and proposed a BCD method, where the digital precoding is handled by the dual method and the analog precoding is addressed by the PDD technique. Then, we extended the proposed algorithm to the sub-connected schemes. In

fact, the proposed design was more computational efficiently than other benchmarks. Simulation results verified the performance of the proposed scheme and provide some meaningful insights: 1) the proposed method obtains close performance with other baselines; 2) hybrid precoder obtains closed performance of the fully-digital schemes; 3) fully-connected scheme is super than the sub-connected case.

References

[1]   J. Zhang, E. Björnson, M. Matthaiou, D. W. K. Ng, H. Yang, and D. J. Love, "Prospective multiple antenna technologies for beyond 5G," *IEEE Journal on Selected Areas in Communications*, vol.38, no.8, pp.1637-1660, 2020. <u>Article (CrossRef Link)</u>

[2]   Z. Wang, M. Li, Q. Liu and A. L. Swindlehurst, "Hybrid Precoder and Combiner Design With Low-Resolution Phase Shifters in mmWave MIMO Systems," *IEEE Journal of Selected Topics in Signal Processing*, vol.12, no.2, pp.256-269, 2018. <u>Article (CrossRef Link)</u>

[3]   X. Yu, J. Shen, J. Zhang, and K. B. Letaief, "Alternating Minimization Algorithms for Hybrid Precoding in Millimeter Wave MIMO Systems," *IEEE Journal of Selected Topics in Signal Processing*, vol.10, no.3, pp.485-500, 2016. <u>Article (CrossRef Link)</u>

[4]   L. Dai, B. Wang, M. Peng, and S. Chen, "Hybrid Precoding-Based Millimeter-Wave Massive MIMO-NOMA With Simultaneous Wireless Information and Power Transfer," *IEEE Journal on Selected Areas in Communications,* vol.37, no.1, pp.131-141, 2019. <u>Article (CrossRef Link)</u>

[5]   S. S. Ioushua and Y. C. Eldar, "A family of Hybrid Analog-Digital Beamforming Methods for Massive MIMO Systems," *IEEE Transactions on Signal Processing,* vol.67, no.12, pp. 3243-3257, 2019. <u>Article (CrossRef Link)</u>

[6]   O. E. Ayach, S. Rajagopal, S. Abu-Surra, Z. Pi, and R. W. Heath, "Spatially Sparse Precoding in Millimeter Wave MIMO Systems," *IEEE Transactions on Wireless Communications,* vol.13, no.3, pp.1499-1513, 2014. <u>Article (CrossRef Link)</u>

[7]   C. Pradhan, A. Li, L. Zhuo, Y. Li, and B. Vucetic, "Hybrid-Precoding for mmWave Multi-User Communications in the Presence of Beam-Misalignment," *IEEE Transactions on Wireless Communications,* vol.19, no.9, pp.6083-6099, 2020. <u>Article (CrossRef Link)</u>

[8]   A. Arora, C. G. Tsinos, B. S. M. R. Rao, S. Chatzinotas, and B. Ottersten, "Hybrid Transceivers Design for Large-Scale Antenna Arrays Using Majorization-Minimization Algorithms," *IEEE Transactions on Signal Processing,* vol.68, pp.701-714, 2020. <u>Article (CrossRef Link)</u>

[9]   S. Gong, C. Xing, V. K. N. Lau, S. Chen, and L. Hanzo, "Majorization-Minimization Aided Hybrid Transceivers for MIMO Interference Channels," IEEE Transactions on Signal Processing, vol.68, pp.4903-4918, 2020. <u>Article (CrossRef Link)</u>

[10] C. Xing, X. Zhao, W. Xu, X. Dong, and G. Y. Li, "A Framework on Hybrid MIMO Transceiver Design Based on Matrix-Monotonic Optimization," *IEEE Transactions on Signal Processing*, vol.67, no.13, pp.3531-3546, 2019. <u>Article (CrossRef Link)</u>

[11] T. Lin, J. Cong, Y. Zhu, J. Zhang, and K. B. Letaief, "Hybrid Beamforming for Millimeter Wave Systems Using the MMSE Criterion," *IEEE Transactions on Communications*, vol.67, no.5, pp.3693-3708, 2019. <u>Article (CrossRef Link)</u>

[12] O. Alluhaibi, Q. Z. Ahmed, E. Kampert, M. D. Higgins and J. Wang, "Revisiting the Energy-Efficient Hybrid D-A Precoding and Combining Design for mm-Wave Systems," *IEEE Transactions on Green Communications and Networking*, vol.4, no.2, pp.340-354, 2020. <u>Article (CrossRef Link)</u>

[13] Y. Cai, F. Cui, Q. Shi, Y. Wu, B. Champagne, and L. Hanzo, "Secure Hybrid A/D Beamforming for Hardware-Efficient Large-Scale Multiple-Antenna SWIPT Systems," *IEEE Transactions on Communications*, vol.68, no.10, pp.6141-6156, 2020. <u>Article (CrossRef Link)</u>

[14] T. Peken, S. Adiga, R. Tandon, and T. Bose, "Deep Learning for SVD and Hybrid Beamforming," *IEEE Transactions on Wireless Communications*, vol.19, no.10, pp.6621-6642, 2020. Article (CrossRef Link)

[15] L. Sun et al., "A Robust Secure Hybrid Analog and Digital Receive Beamforming Scheme for Efficient Interference Reduction," *IEEE Access*, vol.7, pp 22227–22234, 2019. Article (CrossRef Link)

[16] T. Shen, Y. Lin, J. Zou, Y. Wu, F. Shu and J. Wang, "Low-Complexity Leakage-Based Secure Precise Wireless Transmission With Hybrid Beamforming," *IEEE Wireless Communications Letters,* vol.9, no.10, pp.1687-1691, 2020. Article (CrossRef Link)

[17] D. Wu et al., "Secure Hybrid Analog and Digital Beamforming for mmWave XR Communications With Mixed-DAC," *IEEE Journal of Selected Topics in Signal Processing,* vol.17, no.5, pp.995-1006, 2023. https://ieeexplore.ieee.org/document/10192330

[18] X. He and J. Wang, "QCQP With Extra Constant Modulus Constraints: Theory and Application to SINR Constrained Mmwave Hybrid Beamforming," *IEEE Transactions on Signal Processing,* vol.70, pp.5237-5250, 2022. Article (CrossRef Link)

[19] L. Yang, J. Wang, X. Xue, J. Shi and Y. Wang, "Secure Hybrid Beamforming for IRS-Assisted Millimeter Wave Systems," *IEEE Transactions on Wireless Communications,* vol.22, no.8, pp.5111-5128, 2023. Article (CrossRef Link)

[20] Y. Hu, H. Qian, K. Kang, X. Luo and H. Zhu, "Joint Precoding Design for Sub-Connected Hybrid Beamforming System," *IEEE Transactions on Wireless Communications,* vol.23, no.2, pp.1199-1212, 2024. https://ieeexplore.ieee.org/document/10161727

[21] M. R. Akdeniz, Y. Liu, M. K. Samimi, S. Sun, S. Rangan, T. S. Rappaport, and E. Erkip, "Millimeter Wave Channel Modeling and Cellular Capacity Evaluation," *IEEE Journal on Selected Areas in Communications,* vol.32, no.6, pp.1164-1179, 2014. Article (CrossRef Link)

[22] M. M. Naghsh, M. Masjedi, A. Adibi, and P. Stoica, "Max-Min Fairness Design for MIMO Interference Channels: A Minorization-Maximization Approach," *IEEE Transactions on Signal Processing,* vol.67, no.18, pp.4707-4719, 2019. Article (CrossRef Link)

[23] L. Zhang, Y. Wang, W. Tao, Z. Jia, T. Song, and C. Pan, "Intelligent Reflecting Surface Aided MIMO Cognitive Radio Systems," *IEEE Transactions on Vehicular Technology,* vol.69, no.10, pp.11445-11457, 2020. Article (CrossRef Link)

[24] S. H. Hong, J. Park, S-J. Kim, and J. Choi, "Hybrid Beamforming for Intelligent Reflecting Surface Aided Millimeter Wave MIMO Systems," *IEEE Transactions on Wireless Communications,* vol.21, no.9, pp.7343-7357, 2022. Article (CrossRef Link)

[25] A. Kaushik, J. Thompson, E. Vlachos, C. Tsinos, and S. Chatzinotas, "Dynamic RF Chain Selection for Energy Efficient and Low Complexity Hybrid Beamforming in Millimeter Wave MIMO Systems," *IEEE Transactions on Green Communications and Networking,* vol.3, no.4, pp.886-900, 2019. Article (CrossRef Link)

Ying Liu received the M.S. degrees from Nanjing University of Aeronautics and Astronautics, Nanjing, China, in 2011. Since 2008, he has been a lecturer with the College of Information Engineering, Yancheng Institute of Technology, Yancheng, China. His research interests include mmWave communication, cooperative communication, smart radio environments, 5G/6G communication network, unmanned aerial vehicle communication, machine learning, and wireless physical layer security, etc.

Jinhong Bian graduated from the Department of Electronic Engineering of Harbin Institute of Shipbuilding Engineering in July 1991. He is currently a Professor with the College of Information Engineering, Yancheng Institute of Technology, Yancheng, China. His research interests include mmWave communication, smart radio environments, 5G/6G communication network, machine learning, and wireless physical layer security, etc.
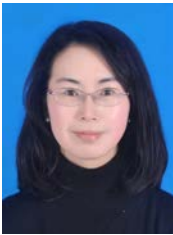
Yuanyuan Wang received the B.S. degrees and M.S. degrees from Soochow University, Suzhou, China, in 2005 and 2008 respectively. She is currently an Associate Professor with the College of Information Engineering, Yancheng Institute of Technology, Yancheng, China. Her research interests include speech recognition, image signal processing, array signal processing, mmWave communication, and 5G/6G communication network, etc.